RIBBON 2-KNOTS, 1+1=2, AND DUFLO'S THEOREM FOR ARBITRARY LIE ALGEBRAS

DROR BAR-NATAN, ZSUZSANNA DANCSO, AND NANCY SCHERICH

ABSTRACT. We explain a direct topological proof for the multiplicativity of Duflo isomorphism for arbitrary finite dimensional Lie algebras. The proof follows a series of implications, starting with "the calculation 1+1=2 on a 4D abacus", using the study of *homomorphic expansions* (aka universal finite type invariants) for ribbon 2-knots, and the relationship between the corresponding associated graded space of *arrow diagrams* and universal enveloping algebras. This complements the results of the first author, Le and Thurston, where similar arguments using a "3D abacus" and the Kontsevich Integral was used to deduce Duflo's theorem for *metrized* Lie algebras; and results of the first two authors on finite type invariants of w-knotted objects, which also imply a relation of 2-knots with the Duflo theorem in full generality, though via a lengthier path.

1. INTRODUCTION

For a finite dimensional Lie algebra $\mathfrak{g}$, the Duflo isomorphism is an algebra isomorphism $\Upsilon : S(\mathfrak{g})^{\mathfrak{g}} \to U(\mathfrak{g})^{\mathfrak{g}}$, where $U(\mathfrak{g})^{\mathfrak{g}}$ and $S(\mathfrak{g})^{\mathfrak{g}}$ are the $\mathfrak{g}$ invariant subspaces for the adjoint action on the universal enveloping algebra and the symmetric algebra. (Recall x is called invariant if $g \cdot x = 0$ for every $g \in \mathfrak{g}$.) The map Υ is given by an explicit formula. The difficulty is in showing that this formula represents a homomorphism, namely that it is multiplicative.

This isomorphism was first described for semi-simple Lie algebras by Harish-Chandra in 1951 [HC]. Kirillov conjectured that a formulation of Harish-Chandra's map was an algebra isomorphism for all finite dimensional Lie algebras. Duflo proved Kirillov's conjecture in 1977 [D], and it is now referred to as Duflo's Theorem. Since then, there have been many proofs of Duflo's theorem using techniques outside the setting of the originally formulated problem. For metrized Lie algebras, a topological proof was found by the first author, Le and Thurston in 2009 [BLT] using the Kontsevich integral and a knot theoretic interpretation of "$1 + 1 = 2$ on an abacus". In this paper we give a new topological proof of Duflo's theorem for *arbitrary finite dimensional Lie algebras* using a "4-dimensional abacus" instead of an ordinary 3-dimensional one.

The Dulfo isomorphism is also implied by the now-proven Kashiwara–Vergne (KV) conjecture [KV]. The KV conjecture states that a certain set of equations has a solution in the group of *tangential automorphisms* of the degree completed free Lie algebra on 2 generators. One can extract the Duflo isomorphism from such a solution. The KV conjecture was proven by [AM] in 2006 using deformation quantization. New proofs exploiting the relationship between the KV equations and Drinfel'd associators were found by Alekseev, Torossian and Enriquez shortly thereafter [AT, AET]. A topological context and solution in terms of the 4-dimensional knot theory of *w-foams* was established by the first two authors in [BD2, BD3]. In this context, the KV-conjecture is equivalent to the existence of a *homomorphic expansion*
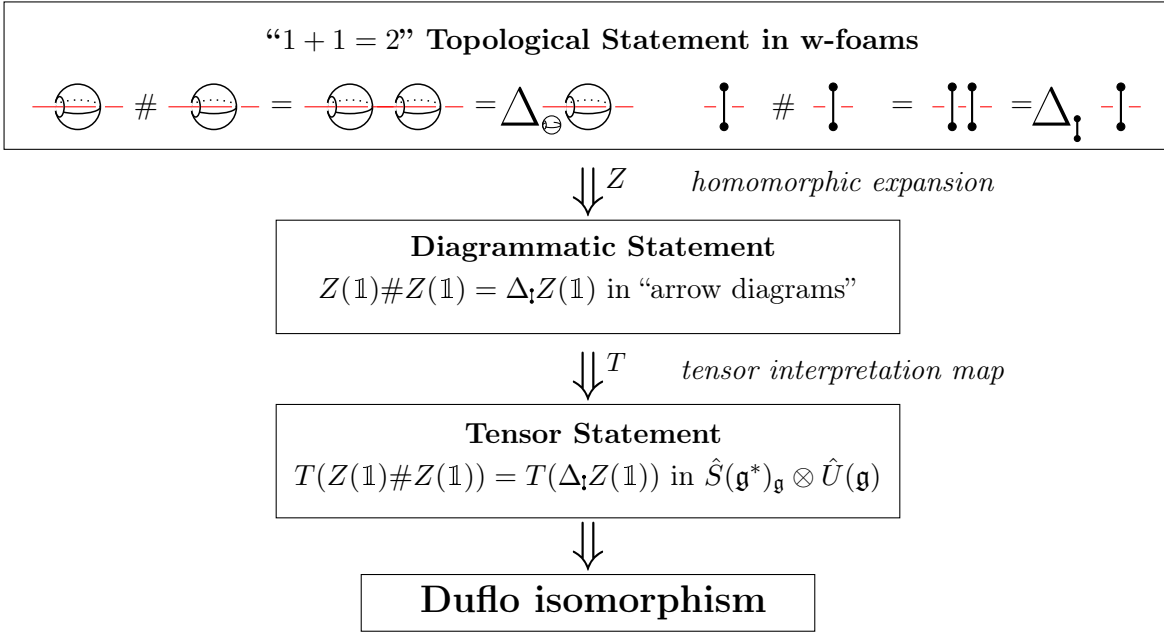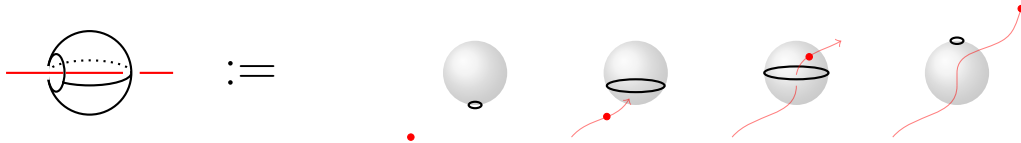
FIGURE 1. The rough sketch of the proof.

FIGURE 2. The threaded sphere as a movie of a circle and a point in $\mathbb{R}^3$.

for w-foams. In this paper, we directly address how such a homomorphic expansion gives rise to a proof of the multiplicativity of the Duflo isomorphism and a formula for Υ, and thus completing a topological proof of the Duflo isomorphism in full generality.

This paper is structured to follow the implications shown in the Figure 1. We start with an intuitive topological statement "$1 + 1 = 2$" and interpret this in the more sophisticated setting of w-foams. Using the homomorphic expansion Z and the tensor interpretation map T, we can re-interpret "$1 + 1 = 2$" as an equality in $\hat{S}(\mathfrak{g}^*)_{\mathfrak{g}} \otimes \hat{U}(\mathfrak{g})$. This will imply that our formulation of the Duflo isomorphism is an algebra homomorphism. The essential ingredient in this process is the homomorphic expansion Z of [BD2, BD3].

2. Understanding the Topological Statement and w-foams

2.1. **"4D Abacus Arithmetic".** The "threaded sphere" or "abacus bead" shown in Figure 2 is a knotted object in $\mathbb{R}^4$, and an element of the space of w-foams studied in [BD2]. To understand this 4D object, we describe it as a sequence of 3D slices, or "frames of a 3D movie". The movie starts with two points A and B. Point B opens up to a circle, A flies through the circle, and B closes to a point again. In 4 dimensions this is a line threaded through a sphere with no intersections; and embedded pair. We depict this object as ⟨threaded sphere symbol⟩ ; this is a *broken surface diagram* in the sense of [CS].
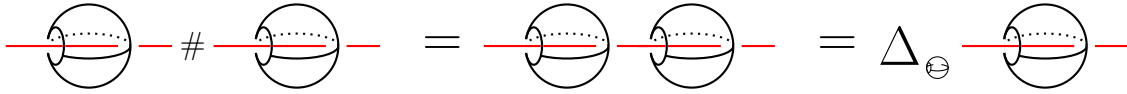
FIGURE 3. "$1 + 1 = 2$" on the 4D abacus.

We can interpret "addition on the 4D abacus" by iteratively threading embedded spheres on a single thread, or in other words, connecting along the threads, as shown in Figure 3. There are two ways to obtain the number 2 from the number 1: by addition – which is represented by iterative threading on the "abacus" thread as above, or by doubling, as explained below.

Assuming the sphere is equipped with a normal vector field (a.k.a. framing, and we will define such a framing later), it makes sense to double the sphere along its framing. This operation will be denoted by $\Delta_\ominus$. For example, given the outward-pointing normal vector field, doubling the sphere results in two concentric spheres. In $\mathbb{R}^4$ two concentric spheres can be separated without intersecting each other. E.g, assume the coordinates are called x, y, z and t, and two concentric spheres lie in the hyperplane $\{z = 0\}$. Then one can continuously move the inner sphere into the hyperplane $z = 1$, followed by moving it to a disjoint t-position from the outer sphere and then back to the $\{z = 0\}$ hyperplane.

Combining this with threading, we obtain that doubling a threaded sphere has the same effect as the connected sum of two threaded spheres, as shown in Figure 3. To simplify notation, we will denote the threaded sphere by $\mathbb{1}$, and write $\mathbb{1}\#\mathbb{1} = \Delta_\ominus\mathbb{1}$.

2.2. **w-foams.** In order to introduce the main ingredient Z, the homomorphic expansion, we need to place the threaded sphere in the more complex space of w-foams. We will briefly describe this space here and for more detail refer to [BD3, Section 2].

The space of w-foams, denoted $\widetilde{wTF}$, is a *circuit algebra*, as defined in [BD2, Section 2.4]. In short, circuit algebras are similar to the planar algebras of Jones [J] but without the planarity requirement for the connection diagrams. For an example of a circuit algebra connection diagram, see Figure 6. Circuit algebras are also close relatives of modular operads. Each generator and relation of $\widetilde{wTF}$ has a local topological interpretation in terms of certain *ribbon knotted tubes with foam vertices and strings* in $\mathbb{R}^4$. Note that one dimensional strands cannot be knotted in $\mathbb{R}^4$, however, they can be knotted *with* two-dimensional tubes. In the diagrams, two-dimensional tubes will be denoted by **thick lines** and one dimensional strings by thin red lines.

With this in mind, we define $\widetilde{wTF}$ as a circuit algebra given in terms of generators and relations, and with some extra operations beyond circuit algebra composition. The generators, relations and operations are explained in detail in Sections 2.2.1 and 2.2.2. The local topological interpretation of the generators and relations provides much of the intuition for this paper.

$$\widetilde{wTF} = CA\left\langle \underbrace{\text{}}_{\text{generators}} \,\middle|\, \underbrace{\begin{matrix}\text{R } 1^s \text{ , R2, R3,}\\ \text{R4, OC, CP}\end{matrix}}_{\text{relations}} \,\middle|\, \underbrace{u_e}_{\text{extra operation}} \right\rangle$$

In [BD3] $\widetilde{wTF}$ appears in its larger unoriented version (includes a *wen* and relations describing its behaviour) and it is equipped with more auxiliary operations (eg punctures, orientation
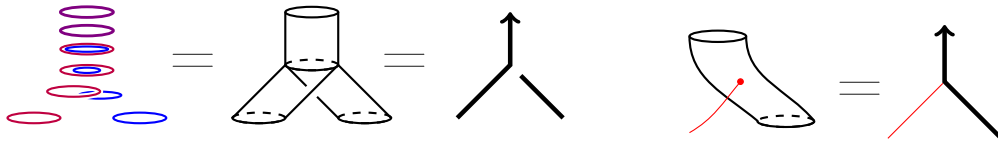
FIGURE 4. The trivalent vertices of $\widetilde{wTF}$.

switches). The expansion Z constructed there is *homomorphic* with respect to all of the operations in the appropriate sense. Here we focus only on orientable surfaces and the operations strictly needed for the Duflo isomorphism – the restriction of the Z of [BD3] is a homomorphic expansion for this structure. In the following sections we will provide brief descriptions of $\widetilde{wTF}$, its associated graded space of arrow diagrams, and the homomorphic expansion, to make this paper more self-contained.

2.2.1. *The generators of* $\widetilde{wTF}$. We begin by discussing the local topological meaning of each generator shown above. For more details, see [BD2, Sections 4.1.1 and 4.5]

Knotted (more precisely, braided) tubes in $\mathbb{R}^4$ can equivalently be thought of as movies of flying circles in $\mathbb{R}^3$. The two crossings – generators 1 and 2 – stand for movies where two circles trade places as the circle corresponding to the under strand flies through the circle corresponding to the over strand entering from below. The bulleted end in generator 3 represents a tube "capped off" by a disk, or alternatively the movie where a circle shrinks to a point and disappears.

Generators 4 and 5 stand for singular "foam vertices", and will be referred to as the positive and negative vertex, respectively. The positive vertex represents the movie shown in Figure 4: the right circle approaches the left circle from below, flies inside it and merges with it. The negative vertex represents a circle splitting and the inner circle flying out below and to the right.

The thin red strands denote one dimensional strings in $\mathbb{R}^4$, or "flying points in $\mathbb{R}^3$". The crossings between the two types of strands (generators 6 and 7) represent "points flying through circles". For example, generator 6 ⤢ stands for "the point on the right approaches the circle on the left from below, flies through the circle and out to the left above it". This explains why there are no generators with a thick strand crossing under a thin red strand: a circle cannot fly through a point.

Generator 8 is a trivalent vertex of 1-dimensional strings in $\mathbb{R}^4$. Finally, generator 9 is a "mixed vertex", in other words a one-dimensional string attached to the wall of a 2-dimensional tube. This is shown in Figure 4.

An important notion for later use is the *skeleton* of a w-foam. We give an intuitive definition here that is is sufficient for this paper; for a formal definition see [BD2, Section 2.4]. In general, viewing knotted objects as embeddings of circles, manifolds, graphs, etc, the skeleton is the embedded object without its embedding. In other words, the skeleton of a knotted object is obtained by allowing arbitrary crossing changes, or equivalently by replacing all crossings with "virtual" (or circuit) crossings. For example, the skeleton of an ordinary knot is a circle. The skeleton of the threaded sphere described above is a sphere and a string. The skeleton of a classical braid on n strands is an element of the permutation group S_n.

2.2.2. *The relations for* $\widetilde{wTF}$. This section is a quick overview of the relations for $\widetilde{wTF}$, which are described in detail in [BD2, Section 4.5]. The list of relations for $\widetilde{wTF}$ is {R1^s, R2, R3, R4, OC, CP}; Figure 5 shows R1^s and OC, and explains CP. All relations have local 4-dimensional
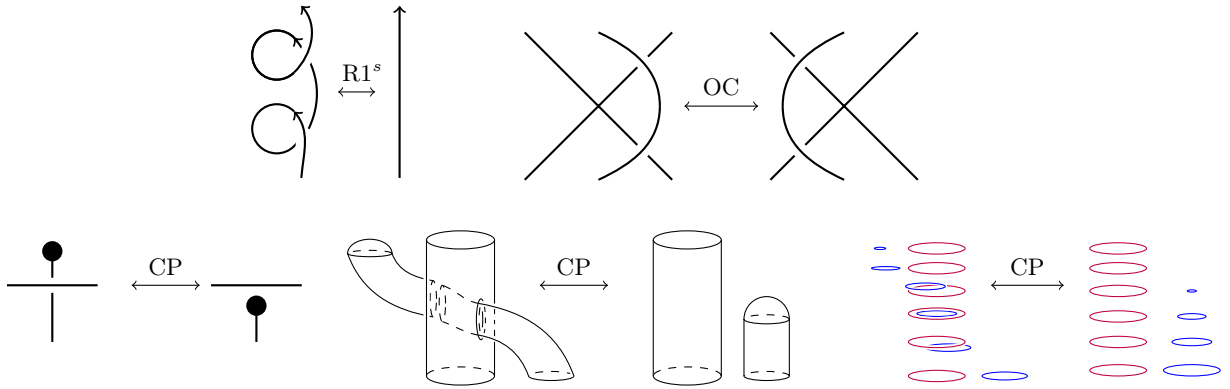
FIGURE 5. The relations R1^s and OC are shown. CP is explained with broken surface diagrams and as a movie of flying circles.
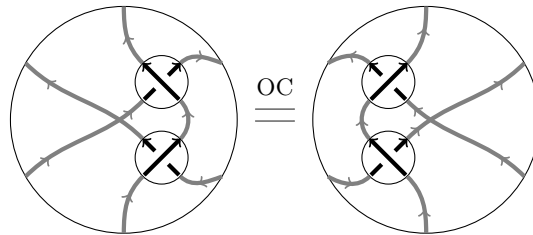

FIGURE 6. The OC relation written as a circuit algebra relation between two crossings.

topological meaning, this is an instructive exercise to verify. R1^s stands for the weak (framed) version of the Reidemeister 1 move; R2 and R3 are the usual Reidemeister moves; and R4 allows moving a strand over or under a vertex. OC stands for *Over-corssings Commute*, and CP for *Cap Pullout*. All relations should be interpreted in all sensible combinations of strand types: tube or string, and all orientations.

Note that all relations are circuit algebra relations. For example, the relation OC is understood as a relationship between two specific circuit diagram compositions of ⤬ and ⤬, as shown in Figure 6.

The circuit algebra $\widetilde{wTF}$ is conjectured to be a Reidemeister theory for *ribbon* knotted tubes in $\mathbb{R}^4$ with caps, singular foam vertices and strings. Here *ribbon* means that the tubes have "filling" in $\mathbb{R}^4$ with only restricted types of singularities, for details see [BD1, Section 2.2.2]. All the relations represent local topological statements: for example, Reidemeister 2 with a thin red bottom strand holds because the movie consisting of a point flying in through a circle and then immediately flying back out is isotopic to the movie in which the point and circle stay in place. However, it is an open question whether the known relations are sufficient. A similar Reidemeister theory has been proven for w-braids,which exhibits a simpler structure than $\widetilde{wTF}$: [BH, Proposition 3.3] and [Gol,Sa]. For an explanation of the difficulties that arise for knots and tangles, see [BD2, Introduction].

2.2.3. *The operations on* $\widetilde{wTF}$. In addition to the circuit algebra structure, $\widetilde{wTF}$ is equipped with a set of auxiliary operations. Of these, in this paper we only use *disc unzip*.
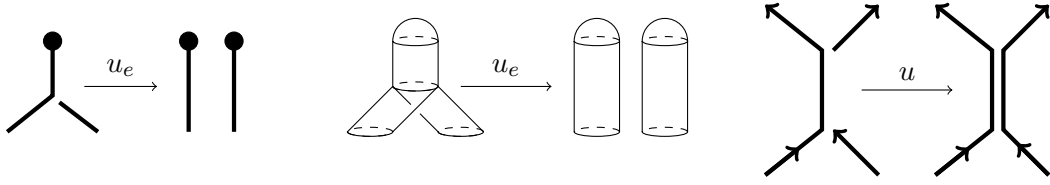
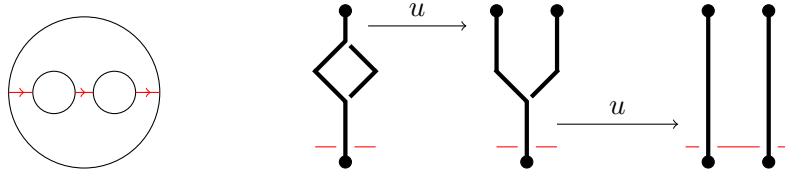FIGURE 7. Disc unzip on the left and middle, strand unzip on the right.

FIGURE 8. On the left, the circuit connection diagram for the connect sum operation, or concatenating along the red strings. On the right, two applications of disc unzips to achieve the doubled sphere.

The *disc unzip operation* u_e is defined for a capped strand labeled by e. Using the blackboard framing, u_e doubles the capped strand e and then attaches the ends of the doubled strand to the connecting ones, as shown Figure 7. Topologically, the blackboard framing of the diagram induces a framing of the corresponding tubes and discs in $\mathbb{R}^4$ via Satoh's tubing map [BD1, Section 3.1.1] and [Sa]. Unzip is the operation "pushing the disc off of itself slightly in the framing direction". See [BD2, Section 4.1.3] for details on framings and unzips.

A related operation not strictly necessary for this proof, *strand unzip*, is defined for strands which end in two vertices of opposite signs, as shown in the right of Figure 7. For the interested reader a detailed definition of crossing and vertex signs is in [BD2, Sections 3.4 and 4.1]. Strand unzip doubles the strand in the direction of the blackboard framing, and connects the ends of the doubled strands to the corresponding edge strands. Topologically, strand unzip pushes the tube off in the direction of the blackboard framing, as before. Note that unzips preserve the ribbon property.

2.3. **Interpreting "$1 + 1 = 2$" in w-foams.** The threaded sphere of Section 2.1 can be described in $\widetilde{wTF}$ by the diagram $\,\overset{-}{\underset{-}{\bullet}}\,$, since a doubly capped tube is in fact a sphere. Recall that the "4D abacus" interpretation of "$1 + 1 = 2$" is $\mathbb{1}\#\mathbb{1} = \Delta_!\mathbb{1}$, where $\mathbb{1}$ is the threaded sphere, and $\Delta_!$ is the doubling of the sphere along a framing.

The connected sum $\#$ operation for the threaded sphere is the circuit algebra composition shown in Figure 8. The doubling $\Delta_!$ can be realized in $\widetilde{wTF}$ using the unzip operation. However, since unzipping a sphere is not one of the operations in $\widetilde{wTF}$, we need to start with a slightly more complex w-foam as shown in Figure 8: we perform two disc unzip operations on a w-foam with two vertices to achieve $\,-\overset{}{||}-\,$. To summarize, the topological statement "$1 + 1 = 2$" expressed in $\widetilde{wTF}$ is shown in Figure 9.

3. Understanding the Diagramatic Statement

3.1. **The associated graded structure $\mathcal{A}^{sw}$.** As in [BD3], the space $\widetilde{wTF}$ is filtered by powers of the augmentation ideal and its associated graded space, denoted $\mathcal{A}^{sw}$, is a space of
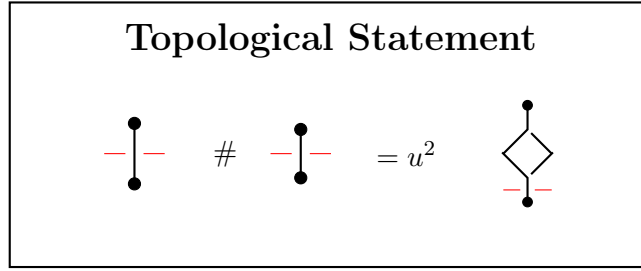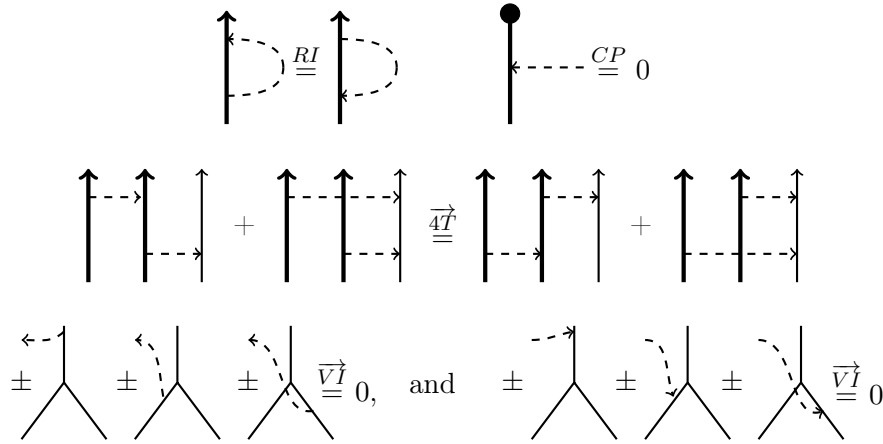
FIGURE 9. The topological statement in w-foams.

FIGURE 10. The relations RI, CP, $\overrightarrow{4T}$ and $\overrightarrow{VI}$.

arrow diagrams on foam skeleta. The *arrows* are drawn as black dashed oriented lines, and the skeleton w-foam elements are drawn with the usual thick black lines and thin red lines. Just like $\widetilde{wTF}$, $\mathcal{A}^{sw}$ is a circuit algebra presented in terms of generators and relations as follows:

$$\mathcal{A}^{sw} = CA \left\langle \left. \underset{1}{\uparrow} , \underset{2}{\uparrow\uparrow} , \underset{3}{\lambda} , \underset{4}{Y} , \underset{5}{\uparrow} , \underset{6}{\lambda} , \underset{7}{\uparrow} \right| RI, CP, \overrightarrow{4T}, \overrightarrow{VI}, TC \left| u_e \right. \right\rangle.$$

Generators 1 and 5 are *single arrows.* A single arrow is a degree 1 element of the associated graded space and represents the difference of a crossing and a non-crossing. The arrow head lies on the under (fly-through) strand of the crossing, and the tail lies on the over strand. All of the other generators of $\mathcal{A}^{sw}$ are *skeleton features* of degree zero. Note that circuit algebra products of the generators will never have an arrow tail on a red string, as red strings never cross over a strand. (Alternatively, we could introduce a relation asserting that arrow tails on red strings equal zero. This is necessary in [BD3] because a 'puncture' operation can give rise to a diagram with a tail on a red string, but not necessary here.) The relations of $\mathcal{A}^{sw}$ are briefly described below, see [BD2, Section 4.2.1] for more detail.

The RI (Rotation Invariance) relation is a consequence of $R1^s$, and CP is the diagrammatic analogue of the CP relation for $\widetilde{wTF}$. Both are shown in Figure 10. The $\overrightarrow{4T}$ and $\overrightarrow{VI}$ relations are also shown in Figure 10. In both cases the ambiguous strands can be either thick black or thin red, but must be consistent through the relation. The $\overrightarrow{VI}$ relation is the diagrammatic analogue of $R4$, and $4T$ has a slightly more complicated topological explanation. The TC (Tails Commute) relation is a consequence of OC and shown in Figure 11.
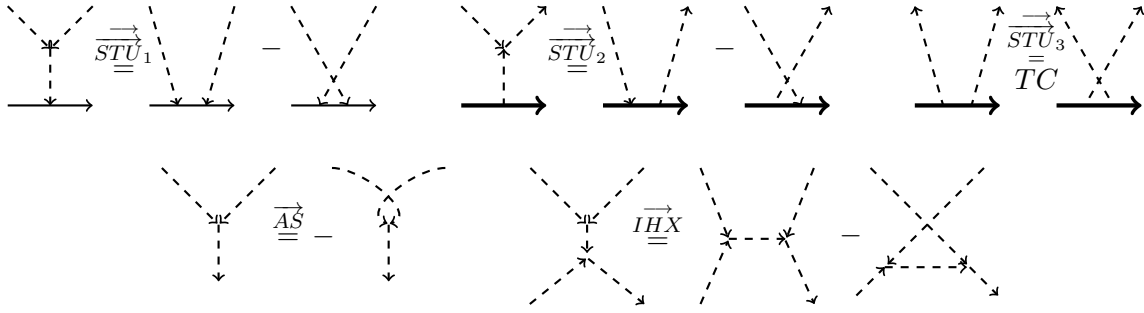
FIGURE 11. The relations $\overrightarrow{STU}$, $\overrightarrow{AS}$ and $\overrightarrow{IHX}$ on $\mathcal{A}^{swt}$.

This presentation of $\mathcal{A}^{sw}$ is intuitive as a mirror of the circuit algebra presentation of $\widetilde{uTF}$. However, for relating $\mathcal{A}^{sw}$ to Lie algebras, it is more useful to use the following isomorphic formulation in terms of *w-Jacobi diagrams*.

A *w-Jacobi diagram* consist of a $\widetilde{uTF}$ skeleton and 'arrow graphs' between the components of the skeleton. An *arrow graph* is an oriented uni-trivalent graph, with the following three properties:

    (1) Univalent vertices are attached to the skeleton.
    (2) Trivalent vertices are equipped with a cyclic orientation.
    (3) The edges are oriented so that every trivalent vertex has two 'in' arrows and one 'out' arrow. This is referred to as the *2-in-1-out* property.

Let $\mathcal{A}^{swt}$ denote the circuit algebra of linear combinations of w-Jacobi diagrams modulo the relations $\overrightarrow{STU}$, CP, RI and $\overrightarrow{VI}$ relations. The $\overrightarrow{STU}$ relation (really three relations) is shown in Figure 11, with TC (Tails Commute) being a degenerate case. The $\overrightarrow{AS}$ and $\overrightarrow{IHX}$ relations, also shown in Figure 11, are consequences of $\overrightarrow{STU}$, and so is $\overrightarrow{4T}$. Once again, ambiguous strands can be either thick black or thin red, consistently throughout the relation. The following theorem is the arrow diagram analogue of a well-known fact about classical "chord diagrams":

Theorem 3.1. *[BD2, Theorem 3.8] The obvious inclusion $\mathcal{A}^{sw} \to \mathcal{A}^{swt}$ is a circuit algebra isomorphism.*

In light of this we drop the t superscript and write $\mathcal{A}^{sw}$ to denote the space of Jacobi diagrams. The advantage of Jacobi diagrams is that trivalent vertices satisfy the same properties as a Lie bracket—this will be made precise using the tensor interpretation map in Section 4.2.

We introduce the following notation: For a w-foam $F \in \widetilde{uTF}$, the circuit algebra $\mathcal{A}^{sw}(S(F))$ is the space of Jacobi diagrams with skeleton $S(F)$, where $S(F)$ is the skeleton of F as defined in Section 2.2. Often we will write $\mathcal{A}^{sw}(F)$ to mean $\mathcal{A}^{sw}(S(F))$.

The associated graded operation of the circuit algebra composition in $\widetilde{uTF}$ is the circuit algebra composition in $\mathcal{A}^{sw}$. As for the (disk) unzip u_e, given a w-foam F with a given strand e, the associated graded unzip operation $u_e : \mathcal{A}^{sw}(F) \to \mathcal{A}^{sw}(u_e(F))$ maps each arrow ending on e to a sum of two arrows, one ending on each of the two new strands which replace e. For example, an arrow diagram with k arrows ending on e – either heads or tails – is mapped to a sum of 2^k arrow diagrams. This sum is suppressed notationally as shown in Figure 12.

3.2. **The Homomorphic Expansion.** As proved by the first two authors in [BD2, BD3], there exists a (group-like) *homomorphic expansion* $Z : \widetilde{uTF} \to \mathcal{A}^{sw}$. An expansion is a
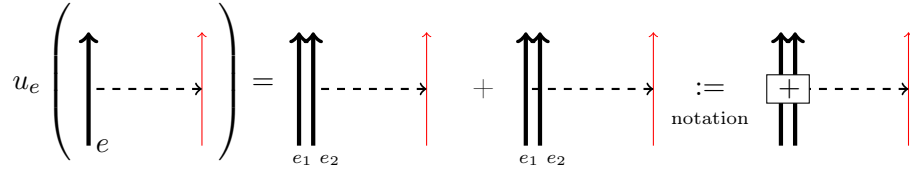
FIGURE 12. Unzipping the strand labeled e, where e_1 and e_2 are the two new strands replacing e.
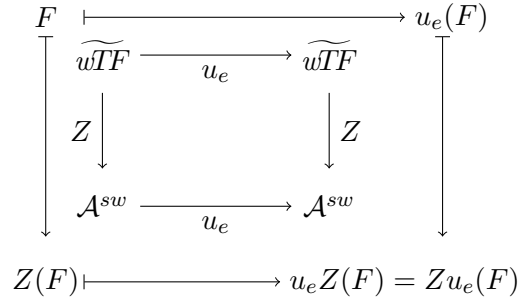

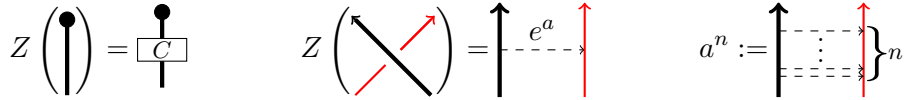FIGURE 13. The commutativity of Z with unzips.

FIGURE 14. Values of Z on generating w-foams.

filtered linear map with the property that the associated graded map $\operatorname{gr} Z : \mathcal{A}^{sw} \to \mathcal{A}^{sw}$ is the identity map on $\mathcal{A}^{sw}$. A homomorphic expansion is an expansion that is a circuit algebra homomorphism and also intertwines each auxiliary operation of $\widetilde{wTF}$ with its arrow diagrammatic counterpart, meaning that the appropriate squares commute. For this paper, the only relevant such operation is the (disk) unzip u_e, the relevant commutative square is shown in Figure 13.

Each generator G of $\widetilde{wTF}$ has an associated skeleton denoted $S(G)$. The map Z sends each generator to an infinite sum of arrow diagrams on the skeleton $S(G)$, that is, $Z(G) \in \mathcal{A}^{sw}(S(G))$. The values of the crossings and the cap are computed explicitly in [BD2,BD3]; to refer to them we use the notation shown in Figure 14. In particular, the Z-value of a crossing of a black strand and a red string is the exponential e^a of an arrow a, to be interpreted as the power series, where a^n is shown in Figure 14.

Since Z is a circuit algebra homomorphism, given the values of Z on the generators, it is straightforward to compute Z of any w-foam F: if F is a circuit composition of some generators $\{G_i\}$, then $Z(F)$ is the same circuit composition of the values $Z(G_i)$.

To understand the diagrammatic statement, we need to discuss the Z-values of the vertices in some detail. By definition, $Z(\lambda) \in \mathcal{A}^{sw}(\lambda)$. Using iterative applications of the relation $\overrightarrow{VI}$, all arrow endings on the vertical strand of λ can be moved to the bottom two strands. This induces an isomorphism $\mathcal{A}^{sw}(\lambda) \cong \mathcal{A}^{sw}(\uparrow\uparrow)$ [BD2]. Thus, $Z(\lambda)$ can be viewed as an
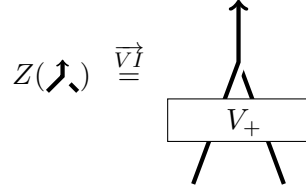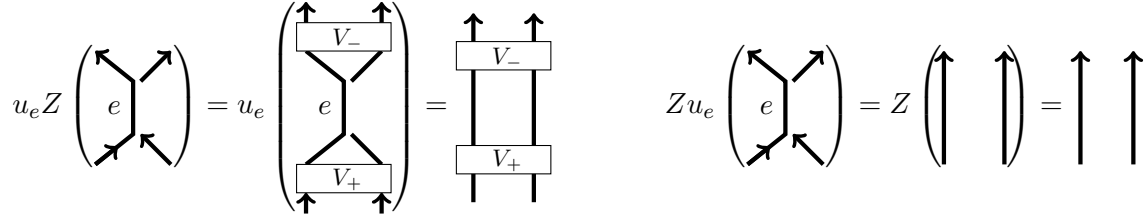
$$Z(\text{↱}) \overset{\overrightarrow{VI}}{=}$$

FIGURE 15. The definition of V_+.

FIGURE 16. Visual proof of Lemma 3.2.

element of $\mathcal{A}^{sw}(\text{↑↑})$ denoted by V_+, as shown in Figure 15. The arrow diagram $V_- = Z(\text{↘↗}) \in \mathcal{A}^{sw}(\text{↑↑})$ is defined similarly.

It is important to note that $\mathcal{A}^{sw}(\text{↑↑})$ is an algebra with multiplication given by vertical concatenation. (In fact, a Hopf algebra with coproduct $\Delta : \mathcal{A}^{sw}(\text{↑↑}) \to \mathcal{A}^{sw}(\text{↑↑}) \otimes \mathcal{A}^{sw}(\text{↑↑})$. The coproduct Δ of an arrow diagram is a sum of all possible ways of attaching each of the connected component of the arrow graph – after removing the skeleton – to one of the tensor factor skeleta. Details on the Hopf algebra structure are in [BD2, Section 3.2].) Let us recall a useful fact from [BD2]:

Lemma 3.2. In $\mathcal{A}^{sw}(\text{↑↑})$, V_+ and V_- are multiplicative inverses, i.e. $V_+ \cdot V_- = 1 = \text{↑↑}$.

Proof. This follows from the fact that Z is homomorphic with respect to the unzip operation, as shown in Figure 16. $\qquad\square$

The following corollary is a crucial ingredient for the diagrammatic statement:

Corollary 3.3. $Z(\text{◇}) = \text{◇}$, that is, the Z-value of this w-foam is trivial, a skeleton with no arrows. $\qquad\square$

3.3. **The diagrammatic statement.** Applying the homomorphic expansion Z to the topological statement of Section 2.3 gives rise to the following equation:

$$Z\left(\text{-↑↑-}\right) = Z\left(\text{-↑-}\right) \# Z\left(\text{-↑-}\right) = u^2 Z\left(\text{◇}\right)$$

Using the notation of Figure 14, we can compute each term of this individually to obtain the final form of the diagrammatic statement, as shown in Figure 17.

4. UNDERSTANDING THE TENSOR STATEMENT

Ultimately we aim to give a proof of the Duflo isomorphism, which is a statement about finite dimensional Lie algebras. Up to this point, the spaces $\widetilde{wTF}$ and $\mathcal{A}^{sw}$ do not depend on

$$Z\left(\;\right) = \quad \xrightarrow{\quad e^a \quad} \qquad u^2 Z\left(\;\right) = u^2 \left(\;\right) \xrightarrow{\quad e^a \quad} = \quad \xrightarrow{\quad e^{a_1 + a_2} \quad}$$

Diagramatic Statement

$$\quad \xrightarrow{e^{a_2}} \quad \xrightarrow{e^{a_1}} \qquad = \qquad \xrightarrow{e^{a_1 + a_2}}$$

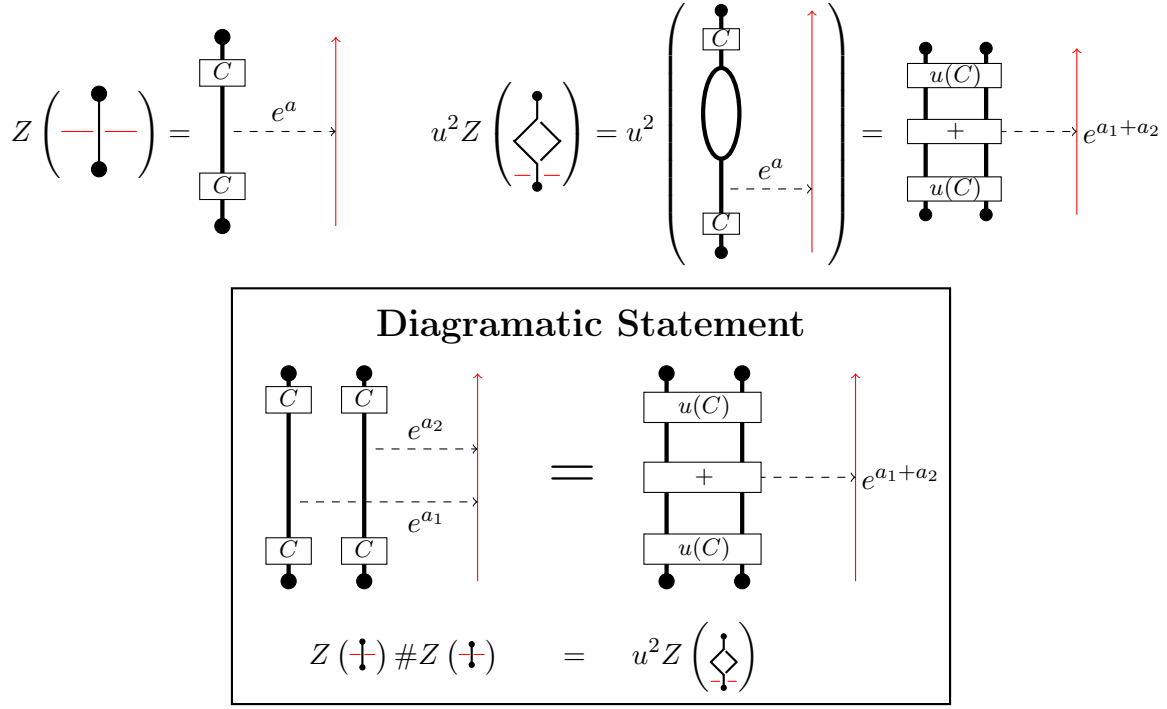$$Z\left(\;\right) \# Z\left(\;\right) \quad = \quad u^2 Z\left(\;\right)$$

FIGURE 17. Computation and conclusion of the Diagrammatic Statement of "1+1 = 2" in $\mathcal{A}^{sw}$. Since tails commute, two caps on a strand can be combined into C^2, and the two unzipped caps can be combined as $u(C)^2 = u(C^2)$.

a Lie algebra, but from here on, we fix a finite dimensional Lie algebra $\mathfrak{g}$ over a field $\mathbb{K}$ of characteristic zero. For each such $\mathfrak{g}$, we define the *tensor interpretation* map

$$T : \mathcal{A}^{sw}(\;) \to \hat{S}(\mathfrak{g}^*)_{\mathfrak{g}}^{\otimes k_1} \otimes \hat{U}(\mathfrak{g})^{\otimes k_2}.$$

Here $\mathcal{A}^{sw}(\;)$ is the space of arrow diagrams on the skeleton of k_1 spheres and k_2 strings, where $k_1, k_2 \in \mathbb{N}$, $\hat{S}(\mathfrak{g}^*)$ is the degree completed symmetric algebra of the linear dual of $\mathfrak{g}$, the subscript $\mathfrak{g}$ denotes co-invariants under the co-adjoint action of $\mathfrak{g}$, and $\hat{U}(\mathfrak{g})$ is the degree completed universal enveloping algebra of $\mathfrak{g}$. (The tensor interpretation map map can be defined on all of $\mathcal{A}^{sw}$ but the target space is more complicated, and $\mathcal{A}^{sw}(\;)$ is enough for our purposes.)

Before defining the map T, we describe the elements in $\mathcal{A}^{sw}(\;)$ in more detail. For even more detail see [BD2, Section3].

4.1. **Elements of $\mathcal{A}^{sw}(\;)$.** The space $\mathcal{A}^{sw}(\;)$ is linearly generated by a relatively "easy" set of arrow diagrams, modulo the relations $\overrightarrow{STU}$ (including TC) and CP. Recall that $\overrightarrow{IHX}$ and $\overrightarrow{AS}$ are implied by $\overrightarrow{STU}$, note that RI is implied by CP here, and $\overrightarrow{VI}$ is not relevant as there are no vertices. With this in mind, a linear generator of $\mathcal{A}^{sw}(\;)$ has the following properties:

(1) Only arrow heads lie on red strings: this is true for every element of $\mathcal{A}^{sw}(\;)$ by definition.

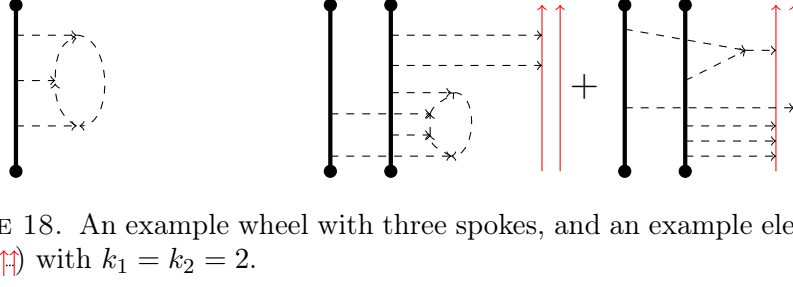FIGURE 18. An example wheel with three spokes, and an example element in
$\mathcal{A}^{sw}(\text{⦙⦙↑↑})$ with $k_1 = k_2 = 2$.

(2) Only arrow tails lie on capped black strands: if an arrow diagram has an arrow head
on a capped strand, one can use iterated $\overrightarrow{STU}$'s and finally CP to express it as a
linear combination of arrow diagrams that don't.
(3) When the skeleton is removed, any connected component of the uni-trivalent arrow
graph belongs to one of the following two classes:
   (a) *Wheels*: an oriented cycle of arrows with a finite number of incoming arrows, or
       "spokes", with all tails lying on capped strands. (The 2-in-1-out property implies
       that all univalent ends must be arrow tails.) See Figure 18 for an example.
       Note that reversing the orientation of an even wheel yields an equivalent arrow
       diagram, while reversing the orientation of an odd wheel produces its negative.
       Hence, from now on we assume all wheels are oriented clockwise.
   (b) *Binary trees* oriented toward a single head, with all tails on caped black strands
       and the head on a red string. A special case is a single arrow. See Figure 18 for
       examples.

4.2. **The Tensor Intpretation Map** T. For a fixed finite dimensional Lie algebra $\mathfrak{g}$, we
now define the *tensor interpretation* map $T : \mathcal{A}^{sw}(\text{⦙⦙↑↑}) \to \hat{S}(\mathfrak{g}_\mathfrak{g}^*)^{\otimes k_1} \otimes \hat{U}(\mathfrak{g})^{\otimes k_2}$. The idea is
that trivalent arrow vertices "represen" the Lie bracket in $\mathfrak{g}$, and the relations in $\mathcal{A}^{sw}$ translate
to Lie algebra axioms and enveloping algebra or symmetric algebra relations.

Denote the structure tensor of the Lie bracket of $\mathfrak{g}$ by $[,]_\mathfrak{g} \in \mathfrak{g}^* \otimes \mathfrak{g}^* \otimes \mathfrak{g}$. Given a basis
$\{b_1, \cdots, b_m\}$ for $\mathfrak{g}$ and the dual basis $\{b_1^*, \cdots, b_m^*\}$ for $\mathfrak{g}^*$, write $[b_i, b_j] = \sum_{k=1}^m c_{i,j,k} b_k$ for
structure constants $c_{i,j,k} \in \mathbb{K}$. Then

$$[,]_\mathfrak{g} = \sum_{i=1}^n c_{i,j,k}\, b_i^* \otimes b_j^* \otimes b_k.$$

Similarly, let $\mathrm{id} \in \mathfrak{g}^* \otimes \mathfrak{g}$ denote the identity map, given by $\mathrm{id} = \sum_{i=1}^m b_i^* \otimes b_i$.

For an arrow diagram D we define $T(D)$ as follows, and as shown in Figure 19:
(1) Place a copy of $\mathrm{id} \in \mathfrak{g}^* \otimes \mathfrak{g}$ on every arrow from a black capped strand to a red strand.
(2) Whenever two trivalent arrow vertices share an edge, divide the edge in half so each
    vertex can be viewed as having three edges "all to themselves".
(3) Place the structure tensor of the bracket $[,]_\mathfrak{g}$ on all trivalent arrow vertices.
(4) The edges that were divided in Step (2) now have an element of $\mathfrak{g}^*$ meeting an element
    of $\mathfrak{g}$. Contract these by evaluating the element of $\mathfrak{g}^*$ on the element of $\mathfrak{g}$ to get a
    constant coefficient. Multiply the constants together. This is illustrated on examples
    in Figures 20 and 21.
(5) What remains is a linear combination of diagrams with elements of $\mathfrak{g}^*$ along the
    black capped strands and elements of $\mathfrak{g}$ along the red strings. Multiplying along the
    orientation of the strands produces an element in the tensor algebra $\mathcal{T}\mathfrak{g}^{*\otimes k_1} \otimes \mathcal{T}\mathfrak{g}^{\otimes k_2}$.
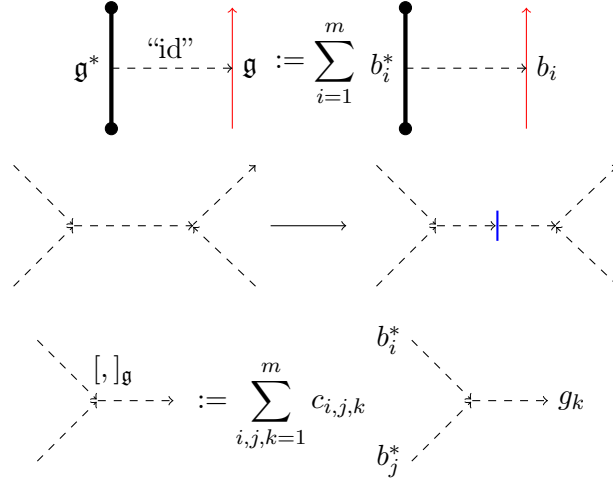
FIGURE 19. Steps (1), (2) and (3) in computing T.
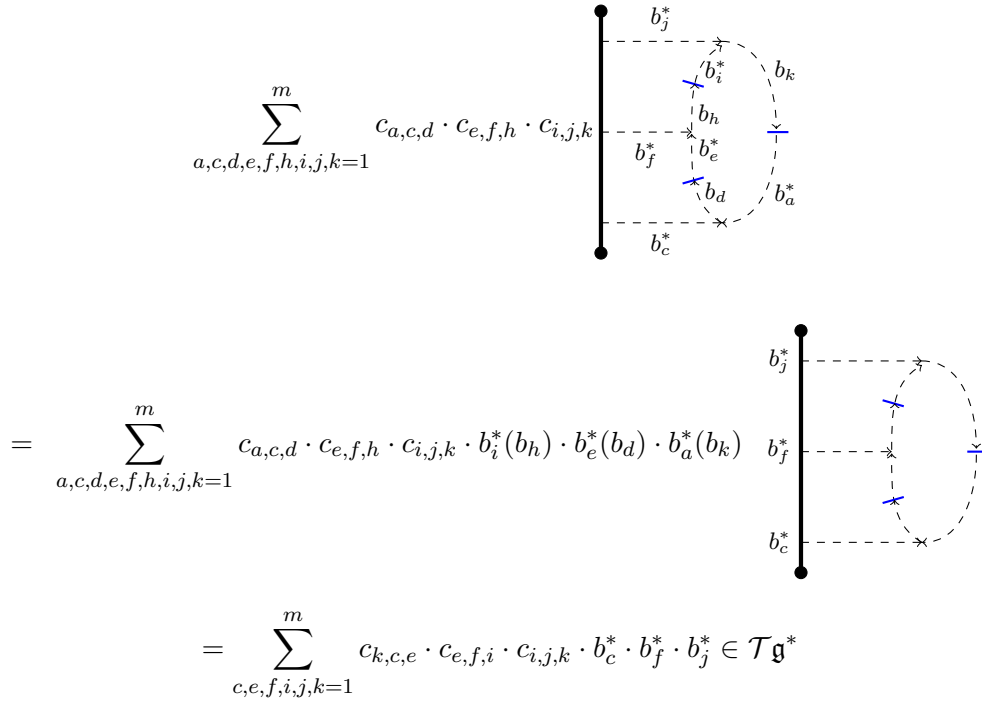
FIGURE 20. Example computation of T for a wheel with three spokes.

Example 4.1. See Figures 20 and 21 for sample computations of T for two arrow diagrams.

Proposition 4.2. *T descends to a well defined map on $\mathcal{A}^{sw}(\uparrow\!\!\uparrow) \to (\hat{S}\mathfrak{g}^*)_{\mathfrak{g}}^{\otimes k_1} \otimes (\hat{U}\mathfrak{g})^{\otimes k_2}$, where $(S\mathfrak{g}^*)_{\mathfrak{g}}$ denotes invariants under the co-adjoint action.*
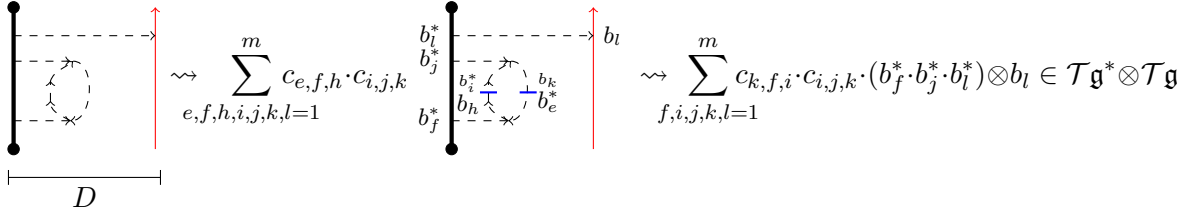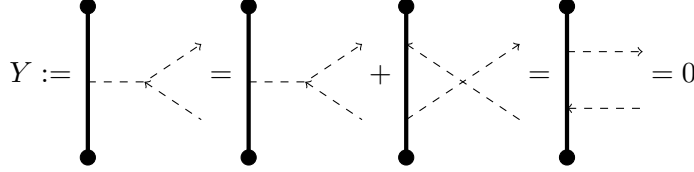
$$\rightsquigarrow \sum_{e,f,h,i,j,k,l=1}^{m} c_{e,f,h} \cdot c_{i,j,k} \qquad\qquad \rightsquigarrow \sum_{f,i,j,k,l=1}^{m} c_{k,f,i} \cdot c_{i,j,k} \cdot (b_f^* \cdot b_j^* \cdot b_l^*) \otimes b_l \in \mathcal{T}\mathfrak{g}^* \otimes \mathcal{T}\mathfrak{g}$$

FIGURE 21. An example for computing T.

$$Y := \qquad = \qquad + \qquad = \qquad = 0$$

FIGURE 22. A single trivalent vertex on a twice-capped strand is zero.

Proof. Given and arrow diagram D, the algorithm above gives an element of $(\mathcal{T}\mathfrak{g}^*)^{\otimes k_1} \otimes (\mathcal{T}\mathfrak{g})^{\otimes k_2}$. We need to show that, modulo the relations of $\mathcal{A}^{sw}(\begin{smallmatrix}\cdot&\cdot\\\cdot&\end{smallmatrix})$, we obtain a well-defined map into $(\hat{S}\mathfrak{g}^*)_{\mathfrak{g}}^{\otimes k_1} \otimes (\hat{U}\mathfrak{g})^{\otimes k_2}$.

Along the red strings, the $\overrightarrow{STU}$ relation translates to the defining relation $[g,h] = gh - hg$ of $U\mathfrak{g}$. Along the capped black strands, there are two further CP relations at the caps.

Due to the first CP relation only tails lie on the capped strands, and the TC relation then translates to the defining relation $\phi\psi = \psi\phi$ of $S\mathfrak{g}^*$. We need to analyze the effect of the second CP relation. First, we assume that only one arrow tail ends on a given capped black strand.

For diagrams which have a single arrow tail ending on a double-capped strand, the second cap relation is equivalent to stating that an arrow diagram where a single trivalent arrow vertex is attached to a capped strand is zero in $\mathcal{A}^{sw}(\begin{smallmatrix}\cdot&\cdot\\\cdot&\end{smallmatrix})$, as shown in Figure 22.

Using the basis $\{b_1, \cdots b_m\}$ and $\{b_1^*, \cdots b_m^*\}$ as before, apply T to the arrow diagram Y of Figure 22. We only know part of the diagram Y, but we can compute the corresponding part of the image. In particular, the structure tensor $\sum_{i,j,k}$ is placed on the single trivalent vertex, the index j does not appear anywhere else, and there are no other factors on the shown capped strand:

$$T(Y) = \sum_{i,j,k} c_{i,j,k} \cdot \underline{\qquad} \cdot b_j^* \otimes \underline{\qquad} = \left(\sum_{j} c_{i,j,k} b_j^* \right) \otimes \sum_{i,k,\dots} \underline{\qquad}$$

Since $Y = 0$ and hence $T(Y) = 0$ for all such diagrams Y, we need

$$\sum_{j} c_{i,j,k} b_j^* = 0 \text{ for all } i, k.$$

A short calculation shows that this is precisely the defining relation for the co-invariant space for the co-adjoint action. In other words the first tensor factor of $T(Y)$ has a well-defined value in $(\mathfrak{g}^*)_{\mathfrak{g}}$.
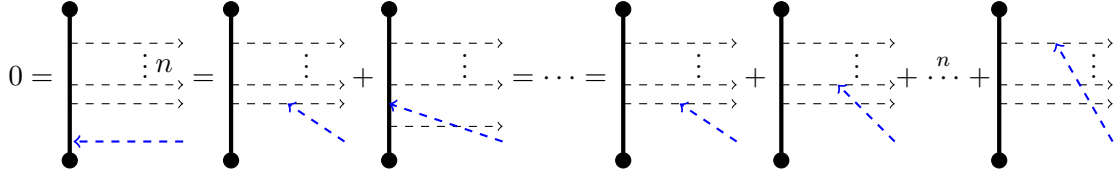
FIGURE 23. Commuting an arrow head up to the top cap, creating a relation on $S\mathfrak{g}^*$.
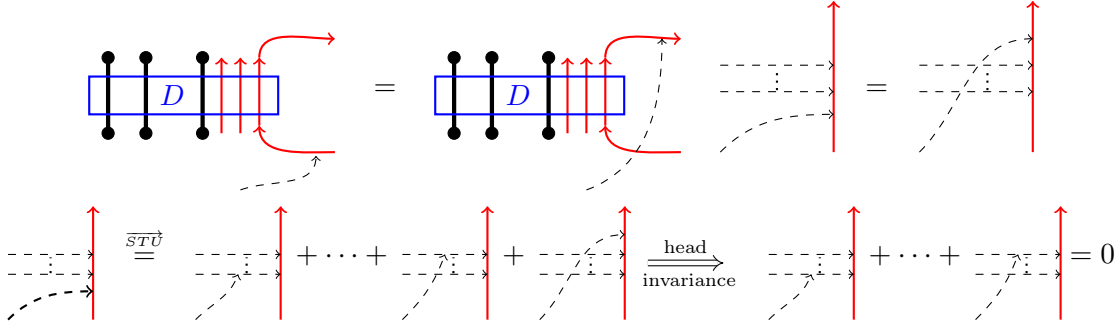

FIGURE 24. Above, the *head invariance* property in $\mathcal{A}^{sw}(\uparrow\uparrow\uparrow\uparrow)$. Below, head invariance and $\overrightarrow{STU}$ implies a relation in $\mathcal{A}^{sw}(\uparrow\uparrow\uparrow)$.

In general, if several arrows end on a double-capped strand, having two CP relations means that any arrow heads can be commuted to either cap and be killed. The resulting relation is shown in Figure 23. After applying T, this translates to exactly how the co-adjoint action of $\mathfrak{g}$ on $\mathfrak{g}^*$ extends to $\hat{S}\mathfrak{g}^*$, hence we obtain the quotient $(\hat{S}\mathfrak{g}^*)_{\mathfrak{g}}$.

$\square$

The following Proposition will play a crucial role later; we present it here as it is based on a similar principle as the proof above:

Proposition 4.3. *The image of T is $\mathfrak{g}$-invariant, where $\mathfrak{g}$ acts via the adjoint action on the i-th $U\mathfrak{g}$ tensor factor, for any $i = 1, ..., k_2$. In other words, $T(D) \in ((\hat{S}\mathfrak{g}^*)_{\mathfrak{g}}^{\otimes k_1} \otimes ((\hat{U}\mathfrak{g}))^{\otimes k_2})^{\mathfrak{g}_i}$ for any $D \in \mathcal{A}^{sw}(\uparrow\uparrow\uparrow\uparrow)$.*

Proof. This follows from the *head invariance* property of arrow diagrams: the implication of this property relevant here is shown in Figure 24; the property in general is discussed in [BD2, Remark 3.14]. In short, attaching an additional arrow head at the bottom of a red strand gives the same result as attaching it at the top. Commuting the arrow head from bottom to top gives a relation similar to the one used in the previous proof and shown in Figure 23.

Now assume that D is an arrow diagram in $\mathcal{A}^{sw}(\uparrow\uparrow\uparrow\uparrow)$, with r arrow heads ending on the i-th red string, for $r, i \in \mathbb{N}$. The tensor $T(D)$ is a sum of terms of the form $P_1 \otimes ... \otimes P_{k_1} \otimes x_1 \otimes ... \otimes x_{k_2}$, where $P_\alpha \in (S\mathfrak{g}^*)_{\mathfrak{g}}$ and $x_\beta \in U\mathfrak{g}$ for $\alpha = 1, ..., k_1$ and $\beta = 1, ..., k_2$. We need to show that for each of these terms x_i is $\mathfrak{g}$-invariant; and enough to show that it is annihilated by each basis element b_s of $\mathfrak{g}$. In such a term, the tensor factor x_i is a product of r basis elements $b_{j_1} \cdot b_{j_2} \cdot ... \cdot b_{j_r}$.
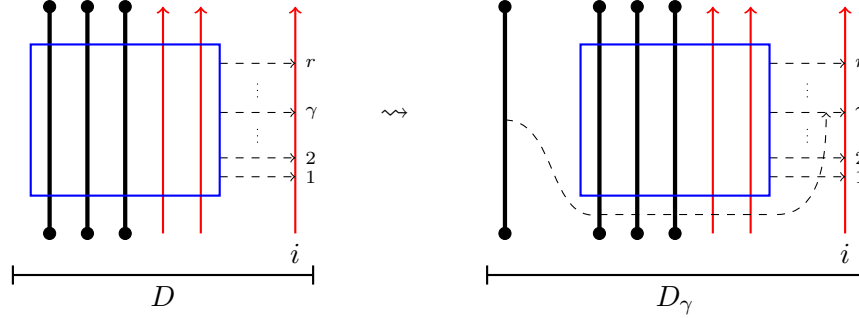
FIGURE 25. Attaching an extra arrow head to the γ-th arrow ending on the i-th red string.

Denote by D_γ the arrow diagram obtained from D by adding an extra balck capped strand, and connecting this with a single arrow to one of the γ-th arrow ending on the i-th red string, as shown Figure 25. The sum $\sum_{\gamma=1}^{r} D_\gamma$ is zero by the head invariance property.

In $T(\sum_{\gamma=1}^{r} D_\gamma)$, the term $P_1 \otimes ... \otimes P_{k_1} \otimes x_1 \otimes ... \otimes x_{k_2}$ of $T(D)$ is replaced with

$$\sum_{s=1}^{m} b_s^* \otimes P_1 \otimes ... \otimes P_{k_1} \otimes x_1 \otimes ... x_{i-1} \otimes \left(\sum_{\gamma=1}^{m} b_{j_1} \cdot ... \cdot [b_s, b_{j_\gamma}] \cdot ... b_{j_2} \cdot ... \cdot b_{j_r}\right) \otimes x_{i+1} ... \otimes x_{k_2}$$

$$= \sum_{s=1}^{m} b_s^* \otimes P_1 \otimes ... \otimes P_{k_1} \otimes x_1 \otimes ... x_{i-1} \otimes (b_s * x_i) \otimes x_{i+1} ... \otimes x_{k_2},$$

where $*$ in the second line denotes the adjoint action. So

$$0 = T\left(\sum_{\gamma=1}^{r} D_\gamma\right) = \sum_{s=1}^{m} b_s^* \otimes \left(b_s *_i T(D)\right),$$

where $*_i$ denotes the adjoint action on the i-th $U\mathfrak{g}$ tensor factor. Hence, $b_s *_i T(D) = 0$ for all $s = 1, ..., m$, and this completes the proof. $\square$

4.3. **The tensor statement.** To obtain the tensor statement, we simply apply the map T to the diagrammatic statement of Figure 17:

$$Z\left(\vcenter{\hbox{}}\right) \# Z\left(\vcenter{\hbox{}}\right) = u^2 Z\left(\vcenter{\hbox{}}\right).$$

Since $Z(\vcenter{\hbox{}})$ is an element of $\mathcal{A}^{sw}(\uparrow\uparrow)$, there exists $\Pi_i \in S(\mathfrak{g}^*)_\mathfrak{g}$ and $W_i \in U(\mathfrak{g})$ so that

$$T(Z(\vcenter{\hbox{}})) = \sum_{i=0}^{\infty} \Pi_i \otimes W_i \in \hat{S}(\mathfrak{g}^*)_\mathfrak{g} \otimes \hat{U}(\mathfrak{g}).$$

The connect sum operation in $\mathcal{A}^{sw}$ is concatenation along the red strings. Under the tensor interpretation map T, this translates to multiplication in $U(\mathfrak{g})$, while the $S(\mathfrak{g}^*)$ components remain separate tensor factors. Hence,

$$T(Z(\vcenter{\hbox{}}) \# Z(\vcenter{\hbox{}})) = \sum_{i,j=0}^{\infty} \Pi_i \otimes \Pi_j \otimes W_i W_j \in \hat{S}(\mathfrak{g}^*)_\mathfrak{g}^{\otimes 2} \otimes \hat{U}(\mathfrak{g}).$$

FIGURE 26. The tensor interpretation map intertwines unzip with comultiplication.

$$
\boxed{
\begin{array}{c}
\textbf{Tensor Statement} \\[4pt]
\displaystyle\sum_{i,j=0}^{\infty} \Pi_i \otimes \Pi_j \otimes W_i W_j = \sum_{i=0}^{\infty} \Delta\Pi_i \otimes W_i
\end{array}
}
$$

FIGURE 27. The tensor statement.

On the right side, the unzip operation sends an arrow ending on the unzipped strand to a sum of two arrows ending on either daughter strand. Under the tensor interpretation map T, this is sent to the Hopf algebra coproduct Δ of $\hat{S}(\mathfrak{g}^*)_{\mathfrak{g}}$ given by $\Delta(\varphi) = \varphi \otimes 1 + 1 \otimes \varphi$ for primitive elements $\varphi \in \mathfrak{g}_{\mathfrak{g}}^*$, as shown in Figure 26. In other words, $T \circ u = \Delta \circ T$.

Examining the right side of the diagrammatic statement in Figure 17, note that it is simply the diagrammatic unzip along the twice-capped strand of $Z(\text{-}|\text{-})$. This is because all arrows of $Z\left(\diamondsuit\right)$ end on the capped strands, none on the "bubble" in the middle. Therefore,

$$
T\left(u^2 Z\left(\diamondsuit\right)\right) = \sum_{i=0}^{\infty} \Delta(\Pi_i) \otimes W_i \in \hat{S}(\mathfrak{g}^*)_{\mathfrak{g}}^{\otimes 2} \otimes \hat{U}(\mathfrak{g}).
$$

In summary, we obtain the Tensor Statement of Figure 27.

5. The Duflo Isomorphism Υ

There is a pairing $\mathfrak{g}^* \times \mathfrak{g} \to \mathbb{K}$ given by the evaluation. This extends to a pairing $S\mathfrak{g}^* \times S\mathfrak{g} \to \mathbb{K}$ in the following way. Given a monomial $\varphi_1 \cdot \ldots \cdot \varphi_k \in S\mathfrak{g}^*$ with $\varphi_i \in \mathfrak{g}^*$ and a monomial of the same degree $x_1 \cdot \ldots \cdot x_k \in S\mathfrak{g}$ with $x_j \in \mathfrak{g}$,

$$
(\varphi_1 \cdot \ldots \cdot \varphi_k)\left(x_1 \cdot \ldots \cdot x_k\right) := \sum_{\sigma \in S_k} \varphi_1(x_{\sigma(1)}) \cdot \ldots \cdot \varphi_k(x_{\sigma(k)}),
$$

where the sum is over all permutations of the k indices. Monomials pair as zero with any monomial of a different degree, and the pairing is then extended bilinearly.

Alternatively, given a basis $\{b_1, ..., b_m\}$ of $\mathfrak{g}$ and dual basis $\{b_1^*, ..., b_m^*\}$ of $\mathfrak{g}^*$, $S\mathfrak{g}$ and $S\mathfrak{g}^*$ are spanned linearly by monomials in the basis elements b_i and b_j^* respectively. The monomial $(b_1^*)^{\alpha_1} \cdot ... \cdot (b_m^*)^{\alpha_m}$ pairs as zero with every monomial in the basis vectors $\{b_i\}$ except $b_1^{\alpha_1} \cdot ... \cdot b_m^{\alpha_m}$, and

$$(5.1) \qquad ((b_1^*)^{\alpha_1} \cdot ... \cdot (b_m^*)^{\alpha_m})\left(b_1^{\alpha_1} \cdot ... \cdot b_m^{\alpha_m}\right) = \prod_{i=1}^{m} \alpha_i!$$

This descends to a pairing $(Sg^*)_{\mathfrak{g}} \times (S\mathfrak{g})^{\mathfrak{g}} \to \mathbb{K}$. For $\Pi \in (Sg^*)_{\mathfrak{g}}$ and $P \in (S\mathfrak{g})^{\mathfrak{g}}$ we will denote the value of this pairing by by $\Pi(P)$. Finally, one can extend to a pairing $(Sg^*)_{\mathfrak{g}}^{\otimes n} \times ((S\mathfrak{g})^{\mathfrak{g}})^{\otimes n} \to \mathbb{K}$ by simply multiplying the pairings of tensor factors. This satisfies the equality

$$(5.2) \qquad \Pi(PQ) = \Delta\Pi(P \otimes Q)$$

for any $P, Q \in (S\mathfrak{g})^{\mathfrak{g}}$, where Δ is the co-product on $(Sg^*)_{\mathfrak{g}}$ induced by the co-product on (Sg^*).

Definition 5.1. We define $\Upsilon : S(\mathfrak{g})^{\mathfrak{g}} \to U(\mathfrak{g})^{\mathfrak{g}}$ by pairing with the first tensor factor of $T(Z(\text{-}\!\!\uparrow\!\!\text{-})) = \sum_{i=0}^{\infty} \Pi_i \otimes W_i$. That is, or $P \in S(\mathfrak{g})^{\mathfrak{g}}$, define

$$\Upsilon(P) := \sum_{i=0}^{\infty} \Pi_i(P) \cdot W_i.$$

The fact that $\Upsilon(P) \in U(\mathfrak{g})^{\mathfrak{g}}$ is a direct consequence of Proposition 4.3.

Theorem 5.2. *The map Υ is an algebra homomorphism.*

Proof. By definition, Υ is linear. The heart of the proof is the multiplicativity of Υ, which is a direct consequence of the Tensor Statement. Let $P, Q \in S(\mathfrak{g})^{\mathfrak{g}}$, then

$$\Upsilon(PQ) = \sum_i \Pi_i(PQ) \cdot W_i \overset{1}{=} \sum_i \Delta\Pi_i(P \otimes Q) \cdot W_i \overset{2}{=} \sum_{i,j} (\Pi_i \otimes \Pi_j)(P \otimes Q) \cdot W_i W_j,$$

$$\overset{3}{=} \left(\sum_i \Pi_i(P) \cdot W_i\right)\left(\sum_j \Pi_j(Q) \cdot W_j\right) = \Upsilon(P)\Upsilon(Q)$$

Here Equality 1 is Equation (5.2) above. Equality 2 is the Tensor Statement, and Equality 3 is the associativity of product. $\qquad\square$

Proposition 5.3. *The map Υ is an algebra isomorphism.*

Proof. In light of Theorem 5.2 we only need to prove that Υ is bijective. This follows from inspection of $T(Z(\text{-}\!\!\uparrow\!\!\text{-}))$; we use the bases $\{b_i\}_{i=1}^{m}$ for $\mathfrak{g}$ and $\{b_i^*\}_{i=1}^{m}$ for $\mathfrak{g}^*$. Recall that $Z(\text{-}\!\!\uparrow\!\!\text{-})$ consists of a value C^2 on the twice-capped strand followed by an exponential e^a of an arrow a from the capped startand to the red string, as shown in Figure 17. Hence,

$$T(Z(\text{-}\!\!\uparrow\!\!\text{-})) = (T(C^2) \otimes 1) \cdot T(e^a).$$

Since $T(a) = \sum_{i=1}^{m} b_i^* \otimes b_i$, we have

$$T(e^a) = e^{\sum_{i=1}^{m} b_i^* \otimes b_i} = \sum_{d=0}^{\infty} \frac{1}{d!}\left(\sum_{i=1}^{m} b_i^* \otimes b_i\right)^d.$$

We will analyse the value C later, for now it is enough to note that since Z is group-like, C is an exponential, and hence $T(C^2) = 1 +$ higher degree terms.

Now let $P \in S(\mathfrak{g})^{\mathfrak{g}}$ be homogeneous of degree d. Observe that $\Upsilon(P)$ is a sum of terms of degree *at most* d, and the highest order term arises from pairing with the term

$$(1 \otimes 1) \cdot \frac{1}{d!} \left(\sum_{i=1}^{m} b_i^* \otimes b_i \right)^d$$

of $\mathrm{T}(\mathrm{Z}(\text{-}\!\!|\text{-}))$. Specifically, P is given by a finite sum $\sum_r b_1^{\alpha_{1,r}} \cdot ... \cdot b_m^{\alpha_{m,r}}$, where $\sum_{i=1}^{m} \alpha_{i,r} = d$ for each r. Then, using Equation 5.1, the highest order term of $\Upsilon(P)$ is

$$\frac{1}{d!} \sum_r \left(\prod_{i=1}^{m} \alpha_{i,r}! \right) W(b_1^{\alpha_{1,r}} \cdot ... \cdot b_m^{\alpha_{m,r}}),$$

where $W(b_1^{\alpha_{1,r}} \cdot ... \cdot b_m^{\alpha_{m,r}})$ denotes the sum of all words in $U\mathfrak{g}$ which use each letter b_i $\alpha_{i,r}$ times. As this sum is non-zero, we have shown that Υ is injective.

Note that Υ is a filtered map: that is, it maps elements of at most degree d in $S(\mathfrak{g})^{\mathfrak{g}}$ to elements of at most degree d in $U(\mathfrak{g})^{\mathfrak{g}}$. Hence, the fact that it is surjective follows from the classical Poincare–Birkhoff–Witt Theorem, which states that $S(\mathfrak{g})^{\mathfrak{g}}$ and $U(\mathfrak{g})^{\mathfrak{g}}$ are isomorphic as filtered vector spaces. $\square$

References

[AM]   A. Alekseev and E. Meinrenken, *On the Kashiwara-Vergne conjecture,* Inventiones Mathematicae, **164** (2006) 615–634, arXiv:0506499.

[AET]   A. Alekseev, B. Enriquez, and C. Torossian, *Drinfeld's associators, braid groups and an explicit solution of the Kashiwara-Vergne equations,* Publications Mathématiques de L'IHÉS, **112-1** (2010) 143–189, arXiv:0903.4067.

[AT]   A. Alekseev and C. Torossian, *The Kashiwara-Vergne conjecture and Drinfeld's associators,* Annals of Mathematics **175** (2012) 415–463, arXiv:0802.4300.

[BD1]   D. Bar-Natan and Z. Dancso, *Finite Type Invariants of W-Knotted Objects I: W-Knots and the Alexander Polynomial,* Alg. Geom. Topol. **16** (2016) 1063–1133.

[BD2]   D. Bar-Natan and Z. Dancso, *Finite Type Invariants of W-Knotted Objects II: Tangles and the Kashiwara-Vergne Problem,* Math. Annalen **367**(3-4) (2017) 1517–1586. arXiv:1405.1955.

[BD3]   *Finite Type Invariants of W-Knotted Objects III: the Double Tree Construction* draft.

[BLT]   D. Bar-Natan, T. Q. T. Le, and D. P. Thurston, *Two applications of elementary knot theory to Lie algebras and Vassiliev invariants,* Geom. Topol. **7-1** (2003) 1–31, arXiv: math.QA/0204311.

[BH]   T. Brendle and A. Hatcher, Configuration Spaces of Rings and Wickets, Comment. Math. Helv. **88** (2013), no. 1, 131–162. arXiv:0805.4354

[CS]   J. S. Carter and M. Saito, *Knotted surfaces and their diagrams,* Mathematical Surveys and Monographs **55**, American Mathematical Society, Providence 1998.

[D]   M. Duflo, *Opérateurs différentiels bi-invariants sur un groupe de Lie*, Ann. Sci. École Norm. Sup. **10** (1977), 265–225.

[Gol]   D. M. Goldsmith, *The Theory of Motion Groups,* Mich. Math. J. **28-1** (1981) 3-17.

[HC]   Harish-Chandra, *On Some Applications of the Universal Enveloping Algebra of a Semisimple Lie Algebra* Trans. Amer. Math. Soc. **70** (1951), 28–96.

[J]   V. F. R. Jones, *Planar algebras I,* arXiv:math/9909027

[KV]   M. Kashiwara and M. Vergne, *The Campbell-Hausdorff Formula and Invariant Hyperfunctions,* Invent. Math. **47** (1978) 249–272.

[Sa]   S. Satoh, *Virtual Knot Presentations of Ribbon Torus Knots*, J. Knot Theory Ramifications **9-4** (2000) 531–542.

Department of Mathematics, University of Toronto, Toronto Ontario M5S 2E4, Canada
Email address: drorbn@math.toronto.edu
URL: http://www.math.toronto.edu/~drorbn

Mathematical Sciences Institute, Australian National University, John Dedman Bldg 26,
Acton ACT 2601, Australia
Email address: zsuzsanna.dancso@anu.edu.au
URL: http://www.math.toronto.edu/zsuzsi

Department of Mathematics, South Hall, Room 6607, University of California, Santa Bar-
bara, CA 93106-3080, United States
Email address: nscherich@math.ucsb.edu
URL: http://www.nancyscherich.com